Photo-induced ring-opening polymerization of trimethylene carbonate-based liquid resins: Towards biodegradable patterned coatings

Nicolas Zivic, Thomas Brossier, Floriane Crestey, Sylvain Catrouillet, Abraham Chemtob, Valérie Héroguez, Patrick Lacroix-Desmazes, Christine Joly-Duhamel, Sébastien Blanquer, Julien Pinaud

Photo-induced ring-opening polymerization of trimethylene carbonate-based liquid resins: Towards biodegradable patterned coatings

Nicolas Zivic [a], Thomas Brossier [a], Floriane Crestey [a], Sylvain Catrouillet [a], Abraham Chemtob [b], Valérie Héroguez [c], Patrick Lacroix-Desmazes [a], Christine Joly-Duhamel [a], Sébastien Blanquer [a], Julien Pinaud [a, *]

[a] *ICGM, Univ Montpellier, CNRS, ENSCM, Montpellier, France*
[b] *Université de Haute-Alsace, CNRS, IS2M, UMR7361, F-68100, Mulhouse, France*
[c] *Univ. Bordeaux, CNRS, Bordeaux INP, LCPO, UMR 5629, F-33600, Pessac, France*

ARTICLE INFO

Keywords:
Photopolymerization
Ring-opening polymerization
Photobase generator
Biodegradable thermosets
Trimethylene carbonate

ABSTRACT

Patterned coatings based on biodegradable crosslinked poly(ester/carbonate) have been prepared by photo-induced ring-opening polymerization of a liquid bifunctional trimethylene carbonate-based monomer using poly (ε-caprolactone) triol as initiator and a guanidine superbase photogenerator activated by irradiation at 385 nm. The influence of various parameters on gel time such as components molar ratios, irradiation time or reaction temperature, has been evaluated by photorheometry. The formulation and experimental conditions offering the shortest gel times were then employed to produce a patterned coating by stereolithography. Sample thickness proves to be independent of irradiation time, but increases with reaction time, thus attesting of a dark polymerization.

1. Introduction

Producing biodegradable materials by a photopolymerization process has been the subject of increased attention over the past ten years [1]. In addition to their environmental benefits, biodegradable photopolymers are in high demand for biomedical products including safe and absorbable adhesives for fast wound closure [2–5], scaffolds for tissue engineering [6–8] or 3D printed implants [9]. To date, the main route to produce such materials relies on the chemical modification of biodegradable natural or synthetic oligomers and monomers to introduce two or more reactive (meth)acrylate reactive functions. After, mixing with a radical photoinitiator, they are generally crosslinked under UV–visible irradiation as thin films in solvent-free systems [1,2,8]. Despite the economic and environmental advantages of this approach, the final product contains a significant fraction of (meth)acrylate units along the chains that are resistant to biodegradation and may accumulate in the environment or in the human body [1]. In addition, unreacted (meth)acrylic fragments may hydrolyze in the human body and subsequently leach into the surrounding tissues, resulting in toxic effects [10]. To achieve complete biodegradability of the product, the repeating units of the final crosslinked photopolymers must also be biodegradable.

To achieve this goal, it is thus necessary to go beyond the conventional radical chain photopolymerization described in the literature. In this regard, an attractive solution would be a step-growth photopolymerization based on multiple thiol-Michael additions as recently described by Zhang et al. [11,12] Though this strategy leads to fast kinetics at room temperature, it also suffers from the toxicity of unreacted (meth)acrylic fragments as mentioned above and from the limited degradability of the thioether repeating units. A more viable alternative is photo-induced ring-opening polymerization (photoROP) of multifunctional cyclic esters and carbonates monomers yielding polymers with biodegradable ester or carbonate repeating units in their backbone [13]. The first example of photoROP was described by Sun et al. in 2008 who reacted ε-caprolactone at 60 °C using a photobase generator (PBG) based on tetraphenylborate salt releasing 1,5,7-triazabicyclo [4.4.0]dec-5-ene (TBD) at 254 nm [14]. Since this study, a variety of PBGs and photoacid generators [15] have been developed for photoROP [16–21]. Nevertheless, most reactions were performed in solution and polymerization rates at ambient temperature are generally slow (90 % conversion after 3 h), preventing the preparation of UV-curable coatings or 3D printed objects. Recently, our group reported a more efficient dual initiating system based on butan-1-ol (initiator) and a ketoprofenate salt of TBD (PBG) that allowed the quantitative conver-

* Corresponding author.
E-mail address: Julien.pinaud@umontpellier.fr (J. Pinaud).

sion of lactide into poly(lactic acid) after only 5 min of irradiation at 254 nm [20]. However, multifunctional lactide-based monomers are generally solid at ambient temperature, which has hindered their wider use in bulk photoROP to produce biodegradable thermoset films [22]. To overcome this issue, we thus have turned our attention towards multifunctional trimethylene carbonate (TMC) monomers, which have the major advantage of being easy to prepare and liquid at room temperature. Our group has already reported the ability of TMC to polymerize at high rates at room temperature [23], but in solution and using non-latent guanidine and amidine based organocatalysts. The goal of the present study is their solvent-free photoROP to prepare biodegradable coatings and patterned films using photolithography.

We thus report herein the UV-induced (385 nm) bulk ROP of a trimethylene carbonate bis-functionalized monomer (DOD-BisTMC) using a biodegradable polycaprolactone-based trifunctional polyol oligomer (PCL-300) as initiator and a TBD salt based on thioxanthone acetic acid (TX-TBD) as PBG [24] to produce biodegradable polyester-carbonate coatings (Scheme 1). Monomer and initiator were both chosen because they lead to PTMC and PCL that are well known to be biodegradable [1]. In a first instance, photorheology was employed to study the effect of various experimental parameters on the progress of the photoROP reaction Then, the most promising formulation was employed to prepare self-standing films, and for the first time, patterned coatings using stereolithography.

2. Experimental

2.1. Instrumentation

2.1.1. Nuclear Magnetic Resonance (NMR) Spectroscopy

^{1}H and ^{13}C were performed at room temperature in 5 mm o.d. tubes on a Bruker AV spectrometer (400 MHz for ^{1}H, 100 MHz for ^{13}C). The ^{1}H chemical shifts are referenced to the solvent peak DMSO (2.50 ppm) and $CHCl_3$ (7.26 ppm). The ^{13}C chemical shifts were determined by ^{13}C-APT experiment and are referenced to the solvent peaks DMSO (39.5 ppm) and $CDCl_3$ (77 ppm). The following abbreviations are used: s = singlet, d = doublet, t = triplet, q = quartet, quint = quintuplet and m = multiplet).

2.1.2. UV/visible spectroscopy

The UV/visible spectrum was recorded at room temperature on a VARIAN Cary 50, using a quartz cuvette of 1 cm path length.

2.1.3. Differential scanning calorimetry (DSC)

DSC experiments were carried out on a NETZSCH DSC200F3. After stabilization at −150 °C, the samples underwent through a heat/cool/heat cycle from −150 °C to 200 °C. All measurements were performed under nitrogen atmosphere fixing the heating and cooling rates at 20 °C/min. Glass transition temperature (T_g) were determined from the second heating cycle of the thermograms.

2.1.4. Rheology

The rheology of the formulations was studied with a HAAKE MARS 60 rheometer (Thermo Scientific) equipped with a light-guided UV-source OmniCure S2000 (λ_{em} = 365–400 nm). An external radiometer OmniCure R2000 was employed to calibrate the intensity of the UV output. The UV intensity was fixed to 30 mW•cm^{-2}. Disposable acrylic and aluminium plates of 20 mm were used respectively as bottom and top geometries (geometry gap of 0.1 mm). All dynamic time sweep experiments were performed employing 1 Hz frequency and 1 % of strain at 30, 35, 40 or 50 °C. The global experiment time was set at 30 min. After 5 min from the beginning, the UV light was turned on and the sample was irradiated for 30 s, 1, 2 or 5 min. Once the UV source was turned off, the measurement continued until the end of the experiment (respectively after 24, 23 and 20 min).

2.2. Materials

All reagents and solvents were purchased from Sigma-Aldrich or VWR and used as received without further purification. Thin layer chromatography (TLC) was done using silica gel on TLC Al foils with fluo-

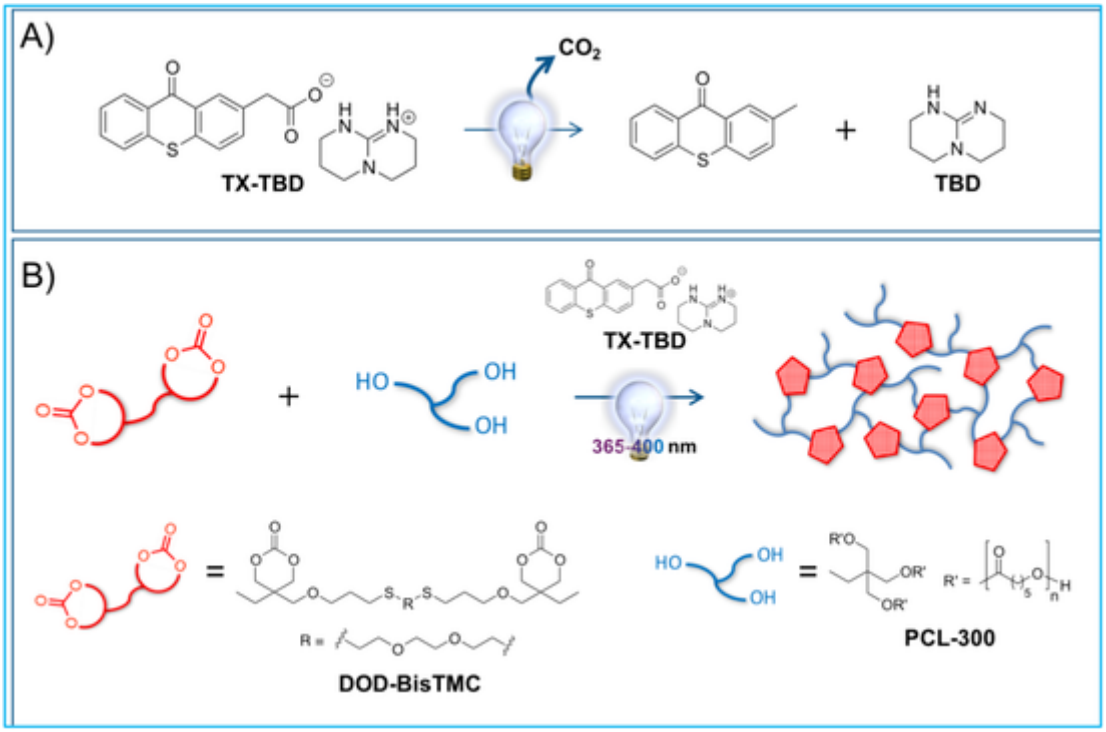

Scheme 1. A) Photodecarboxylation of TX-TBD to generate TBD under 385 nm irradiation; B) Representation of the network formed using DOD-BisTMC as crosslinker and PCL-300 as trifunctional initiator.

rescence indicator (Merck). Chromatography column was performed on a silica gel 60 with particle size of 40–63 μm (VWR).

2.3. Experimental procedures

2.3.1. Preparation of the formulations

In a 5 mL vial equipped with a magnetic stirrer, DOD-bisTMC (1.03 mmol), PCL-300 (0.444, 0.2, 0.1, 0.05, 0.01 or 0 eq.), and TX-TBD (0.0515 mmol, 0.05 eq.) were stirred in DCM until complete solubilization and the solvent was evaporated under vacuum.

2.3.2. Gel content

After reaction, the cross-linked samples (m_0 ~ 100 mg) were washed with a solution of benzoic acid in THF to quench the polymerization. Then, they were placed in fresh THF (20 ml) for 24 h at room temperature. The samples were recovered by filtration, dried at 50 °C during 24 h and finally weighted (m_f). The gel content (%G) was calculated employing the following equation:

$$\%G = \frac{m_f \bullet 100}{m_0}$$

2.3.3. Photocuring test

Photocuring tests were performed using a Digital Light Processing (DLP) Max X43 apparatus from Asiga company by investigating the influence of irradiation time on the rate of polymerization and the precision over the time. Typically, resin deposits were irradiated for different time at 40 °C and the thickness of the generated cured film was measured using a digital thickness gauge (Schmidt, Germany), with 10 μm precision.

2.3.4. Built samples by stereolithography DLP

Coatings were printed at 40 °C from the liquid formulation (PCL-300/DOD-BisTMC/TX-TBD = 10/100/5) using a Digital Light Processing (DLP) Max X43 apparatus from Asiga company that is equipped with a UV light projector irradiating at 385 nm with an irradiance of 20 mW/cm². Grid pattern and institute logo were designed using Rhino3D software. After that, the patterned coatings were gently wiped with a tissue and dried at room temperature.

2.4. Synthetic procedures

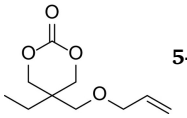

5-((allyloxy)methyl)-5-ethyl-1,3-dioxan-2-one. 2-((allyloxy)methyl)-2-ethylpropane-1,3-diol (26.14 g, 25.9 mL, 0.15 mol, d = 1.01, M = 174.24 g.mol^{-1}) and ethyl chloroformate (48.83 g, 42.8 mL, 0.45 mol, 3 eq., d = 1.14, M = 108.52 g.mol^{-1}) were diluted in anhydrous THF (580 mL) and the solution was cooled at 0 °C. Triethylamine (45.52 g, 62.7 mL, 0.45 mol, 3 eq., d = 0.726, M = 101.19 g.mol^{-1}) was added dropwise during a period of 30 min. The mixture was stirred at room temperature during 2 h. The precipitate of triethylamine hydrochloride was eliminated by filtration. The filtrate was concentrated using a rotary vapor under vacuum. The residue was diluted with ethyl acetate (500 mL) and was washed two times with HCl 1 M (250 mL) and two times with water (250 mL). The organic layer was dried with $MgSO_4$, filtrated and the solvent was removed using a rotary vapor under vacuum. The crude product was purified by distillation under vacuum to afford a colorless oil (21.2 g, 0.106 mol, 71 %). ***^{1}H NMR ($CDCl_3$) δ (ppm):*** 0.91 (t, 3H, ^3J = 7.6 Hz), 1.53 (q, 2H, ^3J = 7.6 Hz), 3.40 (s, 2H), 3.97 (dt, 2H, *J* = 1.3, 5.6 Hz), 4.13 (d, 2H), 4.33 (d, 2H), 5.20 (dq, 1H, *J* = 1.3, 10.4 Hz), 5.26 (dq, 1H, J = 1.6, 17.2 Hz), 5.85 (ddt, 1H, J = 5.6, 10.4, 17.2 Hz). ***^{13}C NMR ($CDCl_3$) δ (ppm):*** 7.3 (CH_3), 23.2 (C_q), 35.3 (CH_2), 68.1 (CH_2), 72.3 (CH_2), 72.7 (CH_2), 117.4 (CH), 134.0 (CH), 148.6 (C=O).

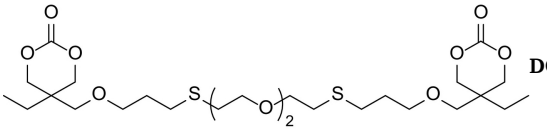

DOD-BisTMC. AIBN (205.3 mg, 1.25 mmol, 0.1 eq., 164.21 g.mol^{-1}) was introduced in DMF (10 mL) and placed under inert atmosphere. 2,2′-(ethylenedioxy)diethanethiol (2.28 g, 2.03 mL, 12.5 mmol, d = 1.12, M = 182.3 g.mol^{-1}) and 5-((allyloxy)methyl)-5-ethyl-1,3-dioxan-2-one (5.0 g, 25.0 mmol, 2 eq., 200.23 g.mol^{-1}) were introduced to the solution and the mixture was stirred at 60 °C during 14 h under inert atmosphere. The resulting solution was poured into water and the product was extracted with ethyl acetate. The combined organic layers were dried with $MgSO_4$, filtrated and the solvent was removed using a rotary vapor under vacuum. The crude product was purified by chromatography column on silica gel (Hexane/AcOEt: 7/3 to 3/7) to afford a colorless oil (4.2 g, 7.20 mmol, 58 %). ***^{1}H NMR ($CDCl_3$) δ (ppm):*** 0.91 (t, 6H, ^{3}J = 7.6 Hz), 1.51 (q, 4H, ^{3}J = 7.6 Hz), 1.84 (m, 4H), 2.61 (t, 4H, ^{3}J = 7.2 Hz), 2.70 (t, 4H, ^{3}J = 6.9 Hz), 3.40 (s, 4H), 3.51 (t, 4H, ^{3}J = 6.1 Hz), 3.64 (m, 8H), 4.12 (d, 4H), 4.31 (d, 4H). ***^{13}C NMR ($CDCl_3$) δ (ppm):*** 7.4 (CH_3), 23.3 (C_q), 29.1 (CH_2), 29.5 (CH_2), 31.3 (CH_2), 35.4 (CH_2), 69.2 (CH_2), 69.9 (CH_2), 70.2 (CH_2), 70.8 (CH_2), 72.8 (CH_2), 148.5 (C=O).

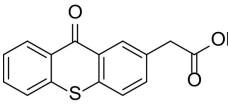

2-(9-oxo-9*H*-thioxanthen-2-yl)acetic acid. Thiosalicylic acid (4.62 g, 30 mmol, 154.86 g.mol^{-1}) was slowly introduced in concentrated H_2SO_4 (95–97 %, 60 mL) and the mixture was stirred at room temperature during 30 min. Phenylacetic acid (12.26 g, 90 mmol, 3 eq., 136.15 g.mol^{-1}) was added dropwise. The mixture was stirred at room temperature during 2 h, at 75 °C during 4 h and at room temperature during 17 h. The resulting solution was carefully poured in boiling water (400 mL) under stirring and the precipitate was collected by filtration. The precipitate was washed two times with boiling water to afford a blue solid (4.61 g, 17.06 mmol, 56 %). ***^{1}H NMR (DMSO-d_6) δ (ppm):*** 3.79 (s, 2H), 7.47–7.89 (m, 5H), 8.36–8.47 (m, 2H).

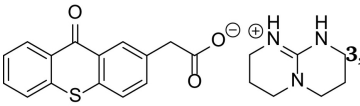

3,4,6,7,8,9-hexahydro-2*H*-pyrimido[1,2-*a*]pyrimidin-1-ium 2-(9-oxo-9*H*-thioxanthen-2-yl) acetate (TX-TBD). TBD (515 mg, 3.70 mmol, 139.2 g.mol^{-1}) was introduced to a solution of 2-(9-oxo-9*H*-thioxanthen-2-yl)acetic acid (1.0 g, 3.70 mmol, 270.3 g.mol^{-1}) in THF (20 mL) and the mixture was stirred at room temperature during 2 h. The resulting precipitate was filtered off and dried under vacuum to afford the product as a yellow solid (950 mg, 2.31 mmol, 63 %). ***^{1}H NMR (DMSO-d_6) δ (ppm):*** 1.84 (quint, 4H, ^{3}J =), 3.12 (t, 4H, ^{3}J =), 3.23 (t, 4H, ^{3}J =), 3.43 (s, 2H), 7.56–7.85 (m, 5H), 8.29–8.49 (m, 2H), 10.02 (bs, 2H). ***^{13}C NMR (DMSO-d_6) δ (ppm):*** 20.4 (CH_2), 37.1 (CH_2), 44.9 (CH_2), 46.1 (CH_2), 125.9 (CH), 126.5 (CH), 126.6 (CH), 127.9 (C_q), 128.4 (C_q), 129.0 (CH), 129.1 (CH), 132.8 (CH), 133.4 (C_q), 134.7 (CH), 136.6 (C_q), 138.0 (C_q), 151.2 (C_q), 178.8 (C_q), 175.6 (C_q).

3. Results and discussion

3.1. Synthesis of DOD-BisTMC, TX-TBD and formulations preparation

In order to obtain a completely biodegradable polymer starting from a liquid formulation composed of an initiator, DOD-BisTMC, and a PBG,

TX-TBD, we selected PCL-300 as initiator since it is a liquid trifunctional polyol with biodegradable caprolactone repeating units. DOD-bisTMC was prepared in two steps using the procedure described by Boutevin et al. (Scheme 2A) [25], while TX-TBD was synthesized in two steps according to the procedure of Liu et al. (Scheme 2B) [24]. Their structure was confirmed by ^{1}H and ^{13}C NMR spectroscopy and the UV/vis absorption spectrum of TX-TBD was recorded in acetonitrile (10^{-5} mol.L^{-1}).

In a first set of experiments, liquid formulations were prepared by directly mixing the three components PCL-300, DOD-BisTMC and TX-TBD and subsequently subjected to 365–400 nm irradiation (30 mW.cm^{-2}) for 10 min. Unfortunately, no curing of the formulations occurred which was attributed to the poor solubility of TX-TBD in the mixture PCL-300/DOD-BisTMX. Consequently, the three components were stirred in DCM until complete solubilization and the solvent was evaporated under vacuum to produce a homogeneous mixture. Under the same irradiation conditions, photocuring occurred, which prompted us to use the same procedure to prepare formulations for the remaining of the study.

3.2. Evaluation of formulations curing by photorheology

Various liquid formulations composed of PCL-300, DOD-BisTMC and TX-TBD were thus prepared and their photocuring reaction monitored by rheometry (Fig. 1). For each set of experiment, monitoring of the curing reaction was fixed at 25 min since formulations taking more time to reach G crossover, corresponding to gel point time, would not be suitable for stereolithography experiments. Table 1 gathers G crossover time and storage moduli (G') for all the studied formulations.

To begin, the amount of TX-TBD was varied between 1 and 5 mol% to determine the amount necessary to obtain the minimum gel point time (Exp 1–3, Table 1). To this end, the molar ratio between the crosslinking agent DOD-BisTMC and PCL-300 was fixed at 100/10, while irradiation time was fixed at 1 min. As can be seen in Fig. 1a, for the three experiments, curing of the formulation continues to occur after UV-irradiation has been stopped. This is opposed to conventional radical photocuring that ceases right after light has been turned off. Nevertheless, such “dark curing" process is not surprising since once TBD has been photoreleased from TX-TBD, it remains an active catalyst for the ROP of DOD-BisTMC. As expected, increasing the amount of TX-TBD resulted in shorter G crossover times, formulations containing 1, 3 and 5 mol% TX-TBD reaching G crossover time after 385 s, 170 s and 67 s respectively. Furthermore, the storage modulus obtained after 25 min with the formulations containing TX-TBD at 3 mol% and 1 mol% were considerably lower compared to the one obtained when TX-TBD was employed at 5 mol%. Consequently, the content of TX-TBD was fixed at 5 mol% for the remaining of the study.

Then, influence of the irradiation time was studied in order to determine the minimum irradiation period required to obtain a fast crosslinking (Fig. 1b). To this end, the formulation with a molar ratio of PCL-300/DOD-BisTMC/TX-TBD = 10/100/5 was exposed to UV irradiation for periods of 30, 60, 120 or 300 s (Exp. 4–7, Table 1). When the formulation was irradiated for 30 s, more than 120 s were necessary to reach G crossover, almost twice the time necessary to reach gel point after 60 s irradiation (67 s). The storage modulus at 25 min (G' = 7100 Pa) was closer to the loss modulus (G") and considerably lower compared to the one of the other formulations. Interestingly, further increase of the irradiation time to 120 and 300 s did not lead to a meaningful decrease of the gel point time, G crossover being reached after 68 and 85 s respectively. It can thus be assumed that after 60 s irradiation, photodegradation of TX-TBD is complete and that TBD is fully released. Accordingly, 60 s was selected as irradiation time for the following experiments.

Because TBD-catalyzed polymerization is known to proceed by a chain-end mechanism, the influence of the relative amount of the PCL-300 initiator and the photobase generator TX-TBD over the reaction rate was also studied. For these experiments, the molar ratio between the cross-linker DOD-BisTMC and the photobase generator TX-TBD was fixed to 100/5, while the molar ratio PCL-300/DOD-BisTMC was varied between 0/100 and 44.4/100 (Exp. 8–13, Table 1; Fig. 1c and d). As ex-

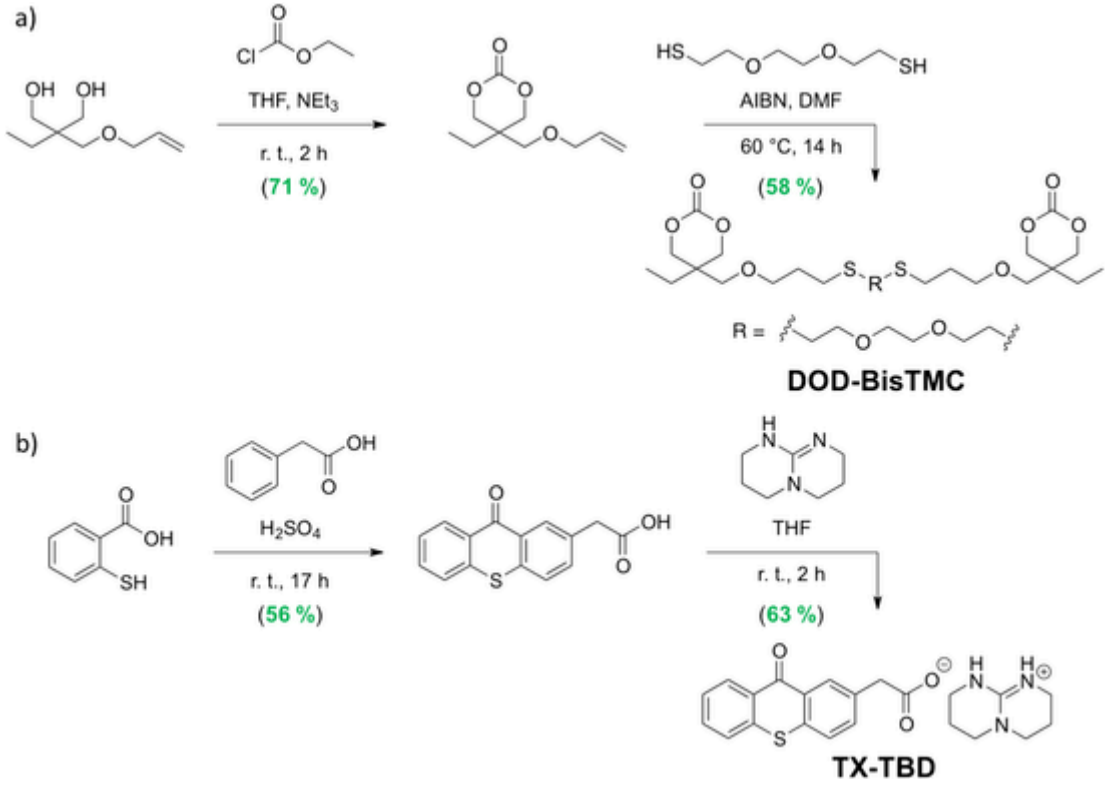

Scheme 2. Synthetic pathways for the achievement of A) DOD-BisTMC and B) TX-TBD.

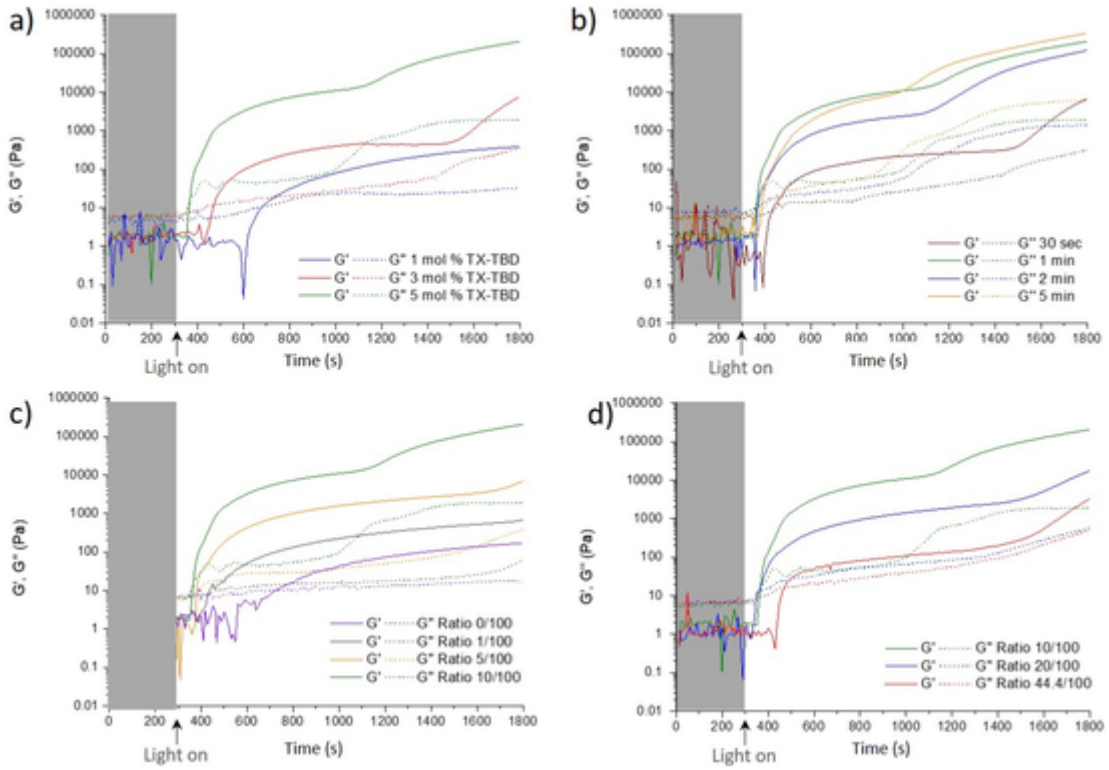

Fig. 1. a) Photopolymerization profiles (λ_{em} = 365–400 nm, irradiation time = 60 s) of formulations with a molar ratio PCL-300/DOD-BisTMC = 10/100 and a molar ratio DOD-BisTMC/TX-TBD = 100/X where X = 1, 3 or 5; b) Photopolymerization profiles (λ_{em} = 365–400 nm) of a formulation PCL-300/DOD-BisTMC/TX-TBD = 10/100/5) for different irradiation times (30, 60, 120 and 300 s); c) and d) Photopolymerization profiles (λ_{em} = 365–400 nm, irradiation time = 60 s) of formulations with a ratio DOD-BisTMC/TX-TBD = 100/5 and with ratios PCL-300/DOD-BisTMC = X/100 where X = 0, 1, 5, 10, 20 or 44.4; d). All experiments where performed at 50 °C.

Table 1
G crossover time and storage modulus (G') after 25 min from the start of UV irradiation for various PCL-300/DOD-BisTMC/TX-TBD formulations submitted to 385 nm irradiation, as function of irradiation time and reaction temperature.

Exp.	Studied parameter	$n_{PCL-300}/n_{DOD-BisTMC}/n_{TX-TBD}$	Irradiation time (s)	Reaction temperature (°C)	G crossover time (s)	G' at 25 min (Pa)
1	PBG content	10/100/5	60	50	67	209,300
2		10/100/3			170	7570
3		10/100/1			385	400
4	Irradiation time	10/100/5	30	50	130	7100
5			60		67	209,300
6			120		68	123,000
7			300		85	338,000
8	PCL-300/DOD-BisTMC ratio	0/100/5	60	50	423	200
9		1/100/5			127	700
10		5/100/5			80	7100
11		10/100/5			67	209,300
12		20/100/5			48	18,100
13		44/100/5			171	3400
14	Reaction temperature	10/100/5	60	50	67	209,300
15				40	193	1400
16				35	452	550
17				30	–	1.5

pected for a ROP proceeding by a chain-end mechanism, increasing the amount of PCL-300 resulted in faster polymerization rates and thus in shorter gel point times. Indeed, formulations with 0/100 and 1/100 PCL-300/DOD-BisTMC molar ratios required long time to reach the G crossover (423 s and 127 s respectively) and, in both cases, yielded gel-like materials, the storage and the loss moduli being similar. For all the other formulations, the obtained materials were solid-like and G crossovers were reached in considerable shorter times of 80, 67 and 48 s for ratios of PCL-300/DOD-BisTMC = 5/100, 10/100 and 20/100, respectively. Interestingly, a higher amount of PCL-300 initiator (PCL-300/DOD-BisTMC = 44.4/100) resulted in an increase of G crossover time to 171 s and in the formation of a material with a much lower storage modulus after 25 min of reaction (G' = 3400 Pa). This phenomenon can be explained by the fact that with such a high content of PCL-300 as compared to the cross-linker, only one DOD-BisTMC can add to each alcohol of the initiator (3 alcohols per PCL-300 initiator). It thus becomes much more difficult to form a network with the remaining TMC units, which results in a longer gel time. In addition, the final material displays many dangling chains and a low crosslinking density, leading to a low storage modulus. Among all the studied formulations, it thus appears that the ratio PCL-300/DOD-BisTMC/TX-TBD ratio of 10/100/5 provides the best compromise between fast photocuring and

final material elastic properties (high G' value).This was further evidenced by the measure of the gel content of the cross-linked material after 25 min of reaction (Table S1). Indeed, despite considerably different storage modulus after 25 min of reaction, almost all the thermosets possessed similar gel contents of 90 %. Only the thermoset obtained from the formulation with a PCL-300/DOD-BisTMC/TX-TBD ratio of 10/100/5 exhibited a high gel content of 98 %.

So far, all experiments have been performed at 50 °C, a temperature supposedly reached by our stereolithography apparatus. Nevertheless, despite all our attempts, our stereolithography apparatus allowed heating of the formulation only up to 40 °C. Thus, we have then examined the influence of temperature on gel point time and final gel content. The photo-induced polymerization of the formulation with a molar ratio PCL-300/DOD-BisTMC/TX-TBD = 10/100/5 was thus conducted at 40 °C, 35 °C or 30 °C (Fig. 2a). As expected, polymerization rates were found to increase with temperature, G crossover time passing from 67 s at 50 °C to more than 400 s at 35 °C, while the formulation remained liquid for the reaction performed at 30 °C. As expected, gel content increased with both reaction time and temperature (Fig. 3). Besides a simple effect of temperature on polymerization kinetics, the difference in gel content and reaction kinetics between the reaction performed at 35 °C and the reaction performed at 30 °C can be explained by the amount of "free" TBD catalyst available in the formulation. Indeed, TX-TBD photodegrades by releasing carbon dioxide that can react reversibly with released TBD to form a TBD-CO_2 adduct that is inactive for ROP [26]. By rising the temperature up to 35 °C, the formation of the TBD-CO_2 adduct can be minored or reversed, thus providing more TBD to catalyze the ROP of DOD-BisTMC.

Finally, the stability of the formulation PCL-300/DOD-BisTMC/TX-TBD (molar ratio 10/100/5) without irradiation was evaluated by rheology. The behavior of the formulation without irradiation is also important in stereolithography because long storage stability of the photocurable formulation is necessary. To assess shelf-stability, the formulation was placed in a rheometer heated at 40 or 50 °C and monitored during 24 h. As observed in Fig. 2b, the formulation shows a good stability at 40 °C with no G crossover within 24 h. At 50 °C the formulation is stable for 13 h, after this time, the storage modulus increases rapidly, leading to a G crossover at 15 h. Consequently, the formulation was found stable enough for conducting stereolithography experiments at 40 °C.

3.3. Glass-transition temperature of obtained materials

The thermal properties of obtained materials with different initiator/cross-linker ratios were determined by DSC (Table S1). No melting transition was observed in any of the thermograms studied, indicating that the thermosets are completely amorphous. The materials presented a glass transition temperature that decreased with increasing amount of initiator, which can be explained considering that increasing the amount of initiator leads to a decrease of cross-linking density (less cross-linker), and thus to polymer chains with higher mobility, lowering the T_g. The material obtained from the formulation with PCL-300/DOD-BisTMC/TX-TBD molar ratio 10/100/5 represents an exception to this trend by having a higher T_g of 3.5 °C. Nevertheless, this can be explained by the higher gel content of 98.1 % as compared to other materials (gel content ≈ 90 %).

3.4. Stereolithography

The formulation displaying the fastest curing kinetics and highest gel content at 40 °C (maximum temperature reached by our stereolithography apparatus), *i.e* PCL-300/DOD-BisTMC/TX-TBD = 10/100/5, was next evaluated in stereolithography process with the aim at producing biodegradable 3D printed objects. In a first instance, to optimize the conditions of processing, a series of photo-curing tests were performed to determine the influence of irradiation time on curing thickness. As shown in Table S2, the layer thickness was almost not impacted by irradiation times. This result is in contrast with the photocuring of acrylate and epoxide resins where the film thickness is directly related to irradiation time [27,28]. Since curing time had no impact on the layer thickness, irradiation time was fixed at 60 s for the remaining of the study.

On the other side, because our approach involves a dark polymerization process that may lead to spreading of the curing beyond the irradiated area, influence of polymerization time after 60 s of irradiation was evaluated. Indeed, the process of layer-by-layer fabrication requires a perfect control of curing with irradiation time to limit the spreading of curing between each layer. Our stereolithography process begins with the printing of a cylinder produced after 60 s of irradiation that displays a thickness of 75 μm and a diameter of 25 μm. As can be seen in Fig. 4, both thickness and diameter of the 3D printed object progressively grow as the object is maintained in the resin tank. This result reflects a distinctive dark polymerization. After 1 h upon photocuring, the thickness increases significantly, over five times from the original thickness. After 5 h of reaction the thickness evolution is even more pronounced by reaching over 13 times its original value. A same trend is logically obtained regarding the diameter of the film. Such continuation of the reaction, or dark polymerization with time is a real limitation for 3D fabrication. However, it does not preclude the fabrication of a patterned layer by lithography. Consequently, stereolithography was used as lithography process to demonstrate the performance of such resin in the fabrication of patterned biodegradable coatings.

Fig. 5 shows a schematic representation of the Computer Aided Design (CAD) used as model to print a layer of the biodegradable ther-

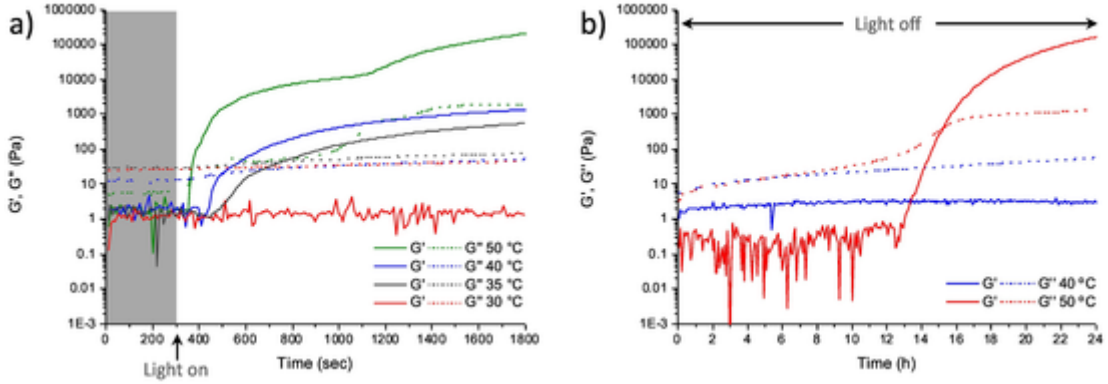

Fig. 2. a) Photopolymerization profiles of a PCL-300/DOD-BisTMC/TX-TBD mixture (molar ratio 10/100/5) under UV exposure (λ_{em} = 365–400 nm, 60 s of irradiation) at different temperatures (30, 35, 40 and 50 °C), b) Polymerization profiles of a PCL-300/DOD-BisTMC/TX-TBD mixture (molar ratio 10/100/5) in the dark at 40 and 50 °C during 24 h.

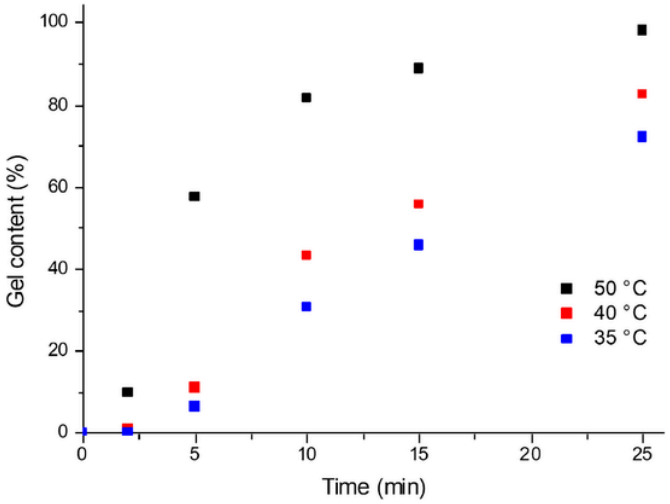

Fig. 3. Evolution of gel content with reaction time for thermosets obtained from the PCL-300/DOD-BisTMC/TX-TBD mixture (molar ratio = 10/100/5) after 1 min of irradiation (λ_{em} = 365–400 nm) and for reaction temperatures of 35, 40 and 50 °C.

moset material by stereolithography. As presented earlier, the minimal thickness that can be reached with this formulation was 80 μm. We thus fixed the irradiation time at 60 s and the post-polymerization time at 15 min to build various photo-crosslinked patterns having an 80 μm thickness by stereolithography. As shown in Fig. 5, patterned coatings have been successfully printed, with high accuracy compared to the CAD model. Fig. 6 displays microscopic photographs of the printed films, which allows to confirm the sharp resolution of the fabricated film, both for right angles and curved morphologies. To the best of our knowledge, this is the first time that a controlled photo-crosslinked layer has been successfully fabricated by stereolithography using a photo-induced ROP approach. Despite thickness increase with time represents a challenge to be overcome to fabricate object by photo-induced ROP, we believe this study opens promising ways to generate fully biodegradable photo-crosslinked structures by stereolithography.

4. Conclusion

For the first time, photo-induced ring-opening polymerization of TMC has been employed to prepare biodegradable poly(ester-carbonate)s crosslinked films *via* a solvent-free curing process. To achieve these results, liquid formulations combining a bis-functionalized TMC monomer (DOD-BisTMC), a polycaprolactone-based trifunctional alcohol initiator (PCL-300) and a photobase generator absorbing at 385 nm (TX-TBD) have been subjected to UVA-irradiation. Among the various experimental parameters tested, reaction temperature and photobase

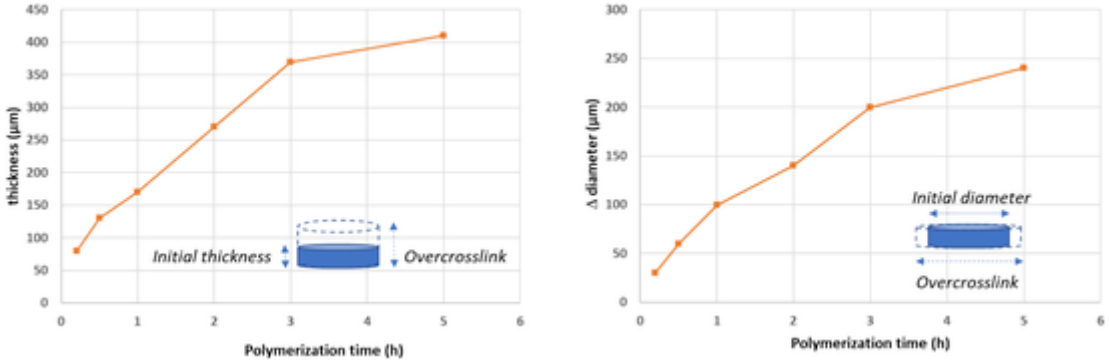

Fig. 4. Evolution with polymerization time of a) thickness and b) Δ diameter (diameter at time t – original diameter) of a photo-cured cylinder obtained after 60 s irradiation of the formulation PCL-300/DOD-BisTMC/TX-TBD = 10/100/5 using a Max X43 DLP apparatus from ASIGA.

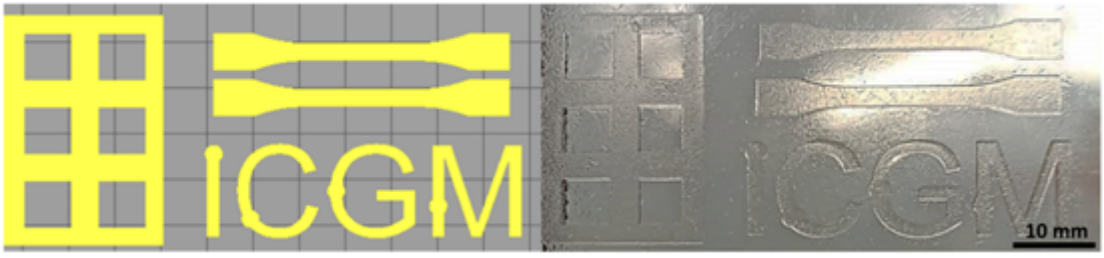

Fig. 5. Images of the STL objects (left) and printed structure (right).

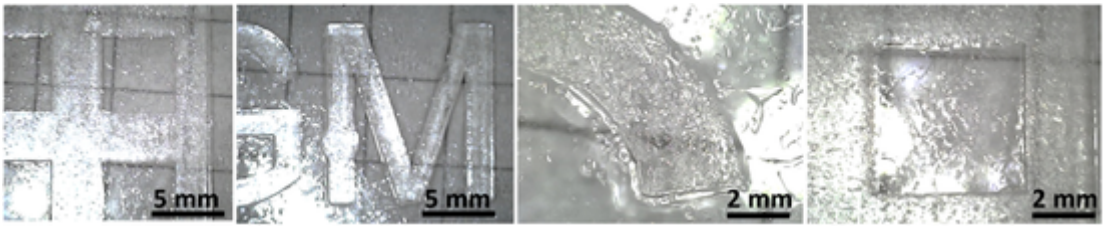

Fig. 6. Microscopic photographs allowing to control the accuracy of dimensions and sharp outlines of the structure printed by irradiation of the PCL-300/DOD-BisTMC/TX-TBD = 10/100/5 formulation, using a Max X43 DLP apparatus from ASIGA.

generator content were found to have the strongest impact on curing kinetics. A dark polymerization process occurred as attested by the reach of G crossover after irradiation ended and by the evidence of curing beyond the irradiated area. Despite this phenomenon, promising patterned coatings were prepared using a stereolithography apparatus. We believe this last result opens the way to the production of fully biodegradable coatings and objects by stereolithography. Current research is underway to limit the spreading of the polymerization beyond the irradiated area and thus to get easy access to well-defined fully biodegradable objects.

Declaration of competing interest

The authors declare that they have no known competing financial interests or personal relationships that could have appeared to influence the work reported in this paper.

Data availability

Data will be made available on request.

Acknowledgement

We would like to dedicate this article to the memory of Dr. Valérie Héroguez who passed away after a long-time illness. Her enthusiasm and wise counsel will be missed. Financial support by French National Research Agency (ANR program: DS0304 2016, contract number: ANR-16-CE07-0016) is gratefully acknowledged.

References

[1] V.S.D. Voet, J. Guit, K. Loos, Sustainable photopolymers in 3D printing: a review on biobased, biodegradable, and recyclable alternatives, Macromol. Rapid Commun. 42 (3) (2021) 2000475.
[2] R.D. O'Rorke, O. Pokholenko, F. Gao, T. Cheng, A. Shah, V. Mogal, T.W.J. Steele, Addressing unmet clinical needs with UV bioadhesives, Biomacromolecules 18 (3) (2017) 674–682.
[3] M. Santos, T. Cernadas, P. Martins, S.P. Miguel, I.J. Correia, P. Alves, P. Ferreira, Polyester-based photocrosslinkable bioadhesives for wound closure and tissue regeneration support, React. Funct. Polym. 158 (2021) 104798.
[4] Y. Zhang, X. Li, Q. Zhu, W. Wei, X. Liu, Photocurable hyperbranched polymer medical glue for water-resistant bonding, Biomacromolecules 21 (12) (2020) 5222–5232.
[5] T. Cernadas, M. Santos, F.A.M.M. Gonçalves, P. Alves, T.R. Correia, I.J. Correia, P. Ferreira, Functionalized polyester-based materials as UV curable adhesives, Eur. Polym. J. 120 (2019) 109196.
[6] E.M. Wilts, A. Gula, C. Davis, N. Chartrain, C.B. Williams, T.E. Long, Vat photopolymerization of liquid, biodegradable PLGA-based oligomers as tissue scaffolds, Eur. Polym. J. 130 (2020) 109693.
[7] G. Weisgrab, O. Guillaume, Z. Guo, P. Heimel, P. Slezak, A. Poot, D. Grijpma, A. Ovsianikov, 3D Printing of large-scale and highly porous biodegradable tissue engineering scaffolds from poly(trimethylene-carbonate) using two-photon-polymerization, Biofabrication 12 (4) (2020) 045036.
[8] N.A. Chartrain, C.B. Williams, A.R. Whittington, A review on fabricating tissue scaffolds using vat photopolymerization, Acta Biomater. 74 (2018) 90–111.
[9] I. Chiulan, E.B. Heggset, Ş.I. Voicu, G. Chinga-Carrasco, Photopolymerization of bio-based polymers in a biomedical engineering perspective, Biomacromolecules 22 (5) (2021) 1795–1814.
[10] G. González, D. Baruffaldi, C. Martinengo, A. Angelini, A. Chiappone, I. Roppolo, C.F. Pirri, F. Frascella, Materials testing for the development of biocompatible devices through vat-polymerization 3D printing, Nanomaterials 10 (9) (2020) 1788.
[11] X. Zhang, W. Xi, G. Gao, X. Wang, J.W. Stansbury, C.N. Bowman, O-nitrobenzyl-based photobase generators: efficient photoinitiators for visible-light induced thiol-Michael addition photopolymerization, ACS Macro Lett. 7 (7) (2018) 852–857.
[12] X. Zhang, X. Wang, S. Chatani, C.N. Bowman, Phosphonium tetraphenylborate: a photocatalyst for visible-light-induced, nucleophile-initiated thiol-Michael addition photopolymerization, ACS Macro Lett. 10 (1) (2021) 84–89.
[13] N. Guy, O. Giani, S. Blanquer, J. Pinaud, J.-J. Robin, Photoinduced ring-opening polymerizations, Prog. Org. Coat. 153 (2021) 106159.
[14] X. Sun, J.P. Gao, Z.Y. Wang, Bicyclic guanidinium tetraphenylborate: a photobase generator and a photocatalyst for living anionic ring-opening polymerization and cross-linking of polymeric materials containing ester and hydroxy groups, J. Am. Chem. Soc. 130 (26) (2008) 8130–8131.
[15] N. Zivic, P.K. Kuroishi, F. Dumur, D. Gigmes, A.P. Dove, H. Sardon, Recent advances and challenges in the design of organic photoacid and photobase generators for polymerizations, Angew. Chem. Int. Ed. 58 (31) (2019) 10410–10422.
[16] Z. Dai, Y. Cui, C. Chen, J. Wu, Photoswitchable ring-opening polymerization of lactide catalyzed by azobenzene-based thiourea, Chem. Commun. 52 (57) (2016) 8826–8829.
[17] C. Fu, J. Xu, C. Boyer, Photoacid-mediated ring opening polymerization driven by visible light, Chem. Commun. 52 (44) (2016) 7126–7129.
[18] F. Eisenreich, M. Kathan, A. Dallmann, S.P. Ihrig, T. Schwaar, B.M. Schmidt, S. Hecht, A photoswitchable catalyst system for remote-controlled (co)polymerization in situ nature, Catalysis 1 (7) (2018) 516–522.
[19] P.K. Kuroishi, A.P. Dove, Photoinduced ring-opening polymerisation of l-lactide via a photocaged superbase, Chem. Commun. 54 (49) (2018) 6264–6267.
[20] E. Placet, J. Pinaud, O. Gimello, P. Lacroix-Desmazes, UV-initiated ring opening polymerization of l-lactide using a photobase generator, ACS Macro Lett. 7 (6) (2018) 688–692.
[21] M.S. Zayas, N.D. Dolinski, J.L. Self, A. Abdilla, C.J. Hawker, C.M. Bates, J. Read de Alaniz, Tuning merocyanine photoacid structure to enhance solubility and temporal control: application in ring opening polymerization, Chemphotochem 3 (6) (2019) 467–472.
[22] P.K. Kuroishi, K.R. Delle Chiaie, A.P. Dove, Polylactide thermosets using a bis (cyclic diester) crosslinker, Eur. Polym. J. 120 (2019) 109192.
[23] F. Azemar, O. Gimello, J. Pinaud, J.-J. Robin, S. Monge, Insight into the alcohol-free ring-opening polymerization of TMC Catalyzed by TBD, Polymers 13 (10) (2021) 1589.
[24] X. Dong, P. Hu, G. Zhu, Z. Li, R. Liu, X. Liu, Thioxanthone acetic acid ammonium salts: highly efficient photobase generators based on photodecarboxylation, RSC Adv. 5 (66) (2015) 53342–53348.
[25] V. Besse, G. Foyer, R. Auvergne, S. Caillol, B. Boutevin, Access to nonisocyanate poly(thio)urethanes: a comparative study, J. Polym. Sci. A Polym. Chem. 51 (15) (2013) 3284–3296.
[26] O. Coulembier, S. Moins, R. Todd, P. Dubois, External and reversible CO2 regulation of ring-opening polymerizations based on a primary alcohol propagating species, Macromolecules 47 (2) (2014) 486–491.
[27] J. Bennett, Measuring UV curing parameters of commercial photopolymers used in additive manufacturing, Addit. Manuf. 18 (2017) 203–212.
[28] B. van Bochove, G. Hannink, P. Buma, D.W. Grijpma, Preparation of designed poly(trimethylene carbonate) meniscus implants by stereolithography: challenges in stereolithography, Macromol. Biosci. 16 (12) (2016) 1853–1863.